New condition monitoring procedure for lifting cranes using motor current signal analysis

M. Lopes Moreira[1], B. Assaad[1], M. Eltabach[1]

[1] Pôle IBV - CETIM s
52 av. Félix Louât, Senlis, France
{marcello.lopesmoreira, bassel.assaad, Mario.eltabach}@cetim.fr}

Abstract

Vibration analysis does not cover all defects able to affect a rotating machine, including those that induce torque or instantaneous rotation speed fluctuations. Indeed the vibrational energy contributions of this type of defects such as a natural and gradual degradation of the gears are often weak. Therefore the appearance of these defects is very difficult to detect from the vibrational energy indicators commonly used in machine condition monitoring. In these conditions, it is often late when the symptoms of failure are reflected in the vibration signal. Several signal processing techniques have emerged to improve the vibration diagnostic result by proposing the use of angular resampling techniques to overcome the difficulties of analyzing non-stationary signals as, for example, velocity fluctuations that can hide the appearance of defects. Other researchers suggest the direct measurement of torque to make the diagnosis, however this technique is intrusive and too expensive. In the recent years there were large interests in diagnosis techniques using motor current signal analysis since these signals are known to be most representative of the torque, easily acquired, not expensive and especially not intrusive. This paper deals with a new diagnostic method based on current signal analysis by associating a simple demodulation technique with an angular resampling technique generally used for vibration signals. Finally the performance of the new method is illustrated through experimental data treating gears wear detection in lifting cranes.

1 Introduction

Nowadays, winches are widely used in construction sites and different industrial applications due to their high reliability and the availability of power converters based on efficient control strategies. In order to increase their performances and their operational lifetime, a permanent condition monitoring of some of their critical parts is necessary. Gears and more precisely planetary gears are extensively used in lifting applications where high speed to torque conversion is required in a small space. Some condition monitoring methodologies have been developed using different types of signals such as temperature, acoustic, electrical, torque or vibration signals. The diagnostic efficiency of these mechanical components using vibration signals has been proved for localized faults as tooth crack. Gears wear detection is not as straightforward as for localized faults because the vibrational energy contributions are weak. In these conditions, gear degradation will induce more torque and instantaneous velocity fluctuations, which arises the vibration level. It is often late when the symptoms of failure are reflected in the vibration signals. Perhaps torque analysis is more suitable to make the diagnosis of these faults; however this technique is intrusive and torque sensors are too expensive. Recently, many methodologies are being developed in diagnosis techniques using motor current signal analysis since these signals are known to be most representative of the torque, easily acquired (already measured in a drive system), and especially not intrusive [1] to [13].

In this paper, the principle of the new method using the electrical current signal is presented in section II. The experimental aspects such as the description of the accelerated lifetime test (ALT) and its instrumentation are presented in the Section III. Results of comparison between the well-known current analysis tech-

nique and the proposed method for monitoring planetary gear of a lifting crane are presented in section IV. Finally, in section V some conclusions and perspectives are given.

2 Principles of the proposed method

The proposed method is based on extracting information from the electrical current signal using the instantaneous speed profile given by a keyphasor.

Figure 1 presents the diagnostic scheme which can be decomposed by three main modules. The first module demodulates the raw current signal. The second one makes an angular transformation of the time demodulated signal using the motor speed profile, while the third module holds the signal analysis in order to extract pertinent condition monitoring features.

2.1 Demodulation module

Modulation is a common phenomenon in condition monitoring of rotating machines using the motor current signal analysis. In fact the current signals are modulated by frequency components related to mechanical phenomenon. The original signal can be one of the three phase current signals assuming that mechanical faults affects in a similar way the three supply currents. These signals can be represented mathematically by equation (1):

$$x(t) = A_m(t).\cos(2\pi f_s t + \phi_m(t)) \tag{1}$$

Where $A_m(t)$ represents the amplitude modulation function ' AMF ' and $\phi_m(t))$ represents the phase modulation function. Performing a demodulation can be done by applying the well-known 'Hilbert transform' on the temporal signal band pass filtered around the supply frequency ' f_s or one of its harmonic'.

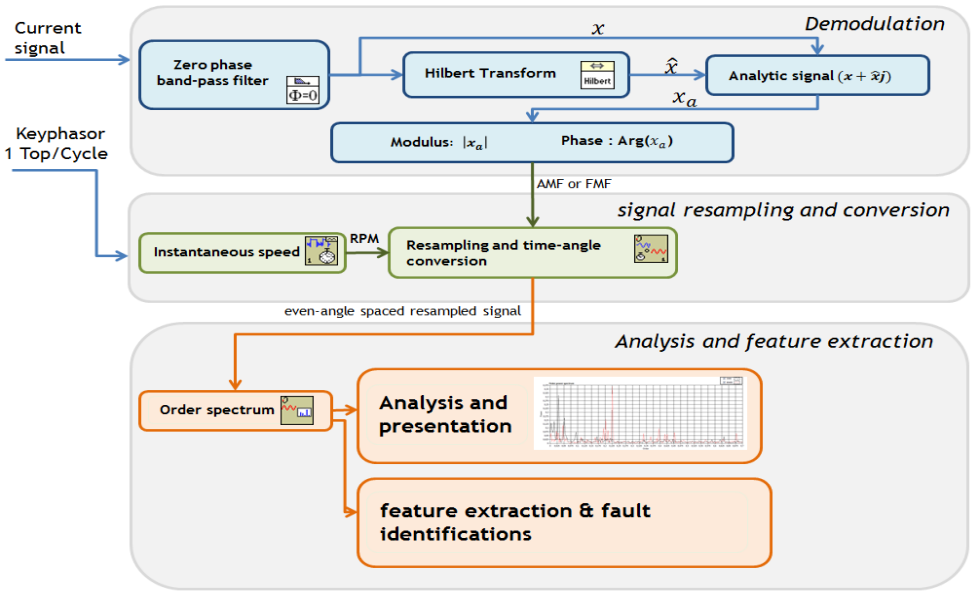

Figure 1: Fault detection scheme

In this case, Equation (1) can be seen as the real part of the 'so-called' analytic signal given by equation (2):

$$x_a(t) = A_m(t).\exp\{j(2\pi f_s t + \phi_m(t)\} \tag{2}$$

Where the Amplitude Modulation Function (AMF) and the Frequency Modulation Function (FMF) can be calculated respectively by equations (3) and (4):

$$AMF = \left| x_a(t) \right| \tag{3}$$

$$FMF = \frac{1}{2\pi}\frac{d\phi_m(t)}{dt} = \frac{1}{2\pi}\frac{d}{dt} Arg\left[x_a(t).e^{-j2\pi f_c t} \right] \tag{4}$$

The modulus of the analytical signal corresponds to the amplitude demodulated signal. Note that, in our paper, we only treat the amplitude demodulation scheme.

The second module makes an angular transformation of the time demodulated signal using the motor speed profile. In fact, the motor velocity is not constant even in the so-called stationary period. In certain cases, this variation can lead to smearing in spectrums which can hide faults signatures. In order to make an accurate diagnosis, angular resampling is a must. Therefore, the latter is calculated utilizing the keyphasor signal (8 tops/motor cycle). The instantaneous velocity is then calculated and an interpolation technique is applied in order to better estimate the angular demodulated signal.

The third module holds the signal analysis in order to extract pertinent fault features. Indeed, order spectrums are computed with the purpose of making signal comparison between healthy and faulty conditions. At this stage, condition monitoring indicators can be extracted in order to identify the machines defects.

2.2 Angular resampling

Generally, the rotational speed of the machine is subjected to speed fluctuations, so that it might be complicated to track the fault characteristic frequencies which also fluctuate. In order to overcome this problem we propose to represent the current signal with respect to the rotational angle of the shaft 'θ'. This consists in substituting the temporal sampling of the signal *x(t)* to an angular sampled signal $x_a(\theta)$. In practical terms, the angular resampling operation is a transformation which replaces a series of samples spaced by a constant period of time T_s with a series of samples spaced by a constant period of angular sampling θ_s. At the end of this operation, angular signals are represented by a constant number of samples by machine cycle regardless of the rotational speed of the machine.

The procedure of angular resampling is shown in Figure 2. The first step is to define an angular resampling grid $\{\theta_n\}$. In the second step, an evaluation of the temporal instants $t[\theta_n]$corresponding to the grid designed in the first step must be done by doing an interpolation. Several methods exist in the literature in order to accomplish this interpolation. We used the well-known cubic spline method. The evaluation of the angular signal values $x_a[\theta_n]$ is done by using also the same interpolation scheme.

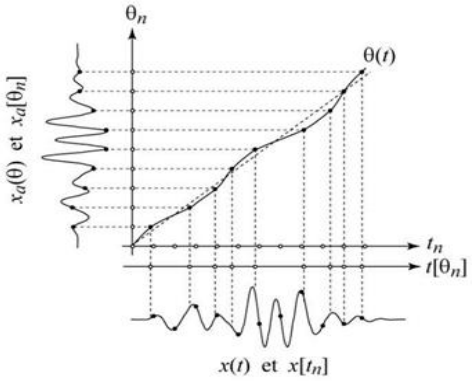

Figure 2: Angular resampling procedure

2.3 *Analysis and feature extraction*

The decomposition of the angular signal along the order axis is accomplished using the Fast Fourier Transformation (FFT). This fast algorithm calculates the discrete Fourier transform of a block of N samples of data *y[N]* and gives an order spectrum *Y(k)* of N orders lines as shown in equation (5).

$$Y(k) = \frac{1}{N}\sum_{n=0}^{N-1} y(n)\exp(-j2\pi kn/N) \quad (5)$$

The frequency index *k* represents the order frequency ($k.\Delta ord$), where $.\Delta ord$ is the line spacing or the order resolution. The record length N gives directly the Δord value ($\Delta ord = f_{sp}/N$) where f_{sp} is the angular sampling frequency. Analysis techniques based on selected spectral lines reflect particular frequencies generated by a certain mechanical component. Such frequencies are gear mesh frequencies (GMF), planet pass frequency (PPF) and planet carrier frequencies. Spectral component amplitude or the sum of several ones can then be used as condition monitoring indicators.

3 EXPERIMENTAL SET UP

Figure 3 shows a global view of the lifting crane used in the accelerated lifetime test (ALT). A key phasor (8 impulses / revolution) is used to compute the instantaneous speed profile. The load is pulled by the winch drum which transmits the torque to the planetary gear. The latter owns two stages with two different reducing factors of 7.25 and 5 respectively. The first planetary gear stage is directly connected via its input shaft to the motor's rotor and its rotating planet carrier is connected to the sun gear shaft of the second gear stage. Figure 4 shows the mechanical drawing of the two staged planetary gear used in the ALT. Currents are measured by using probes installed on the three motor supply cables, see Figure 5.

The load levels applied to the winch during the test period are relatively high compared to real life operating conditions. In addition, no maintenance is performed (no oil change or bearing lubrication) in order to accelerate the winch degradation. The lifetime test began on September 2008 and on February 2012 gear degradation has been clearly revealed by an oil analysis and inspections see Figure 6.

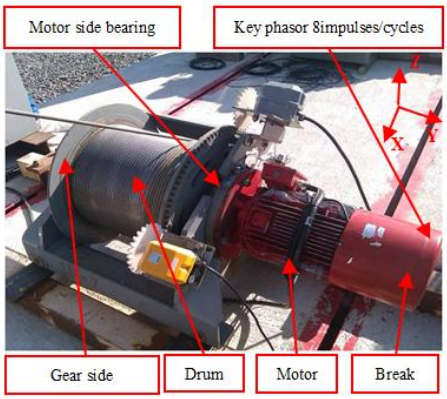

Figure 3:. Benchmark global view

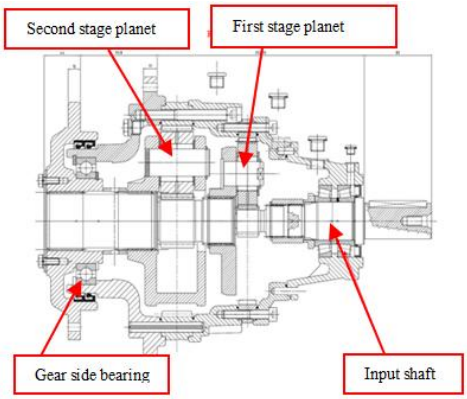

Figure 4:. Benchmark planetary gear

Figure 5: Current probes installed on the motor supply cables

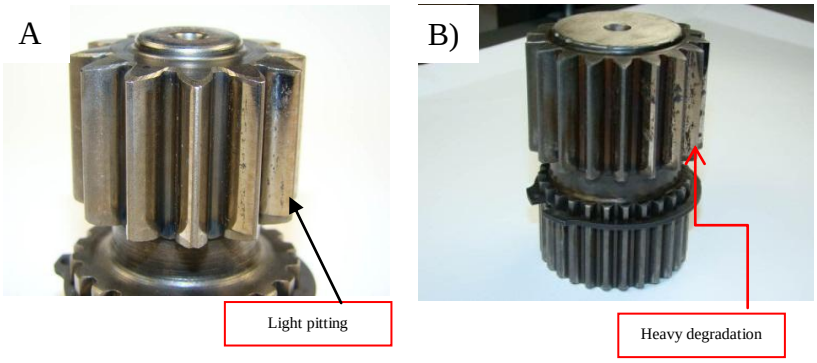

Figure 6: Sun gears inspection A) first stage B) second stage

In the next paragraph we will investigate the ability of the new condition monitoring method to detect the gear degradation. Table 1 gives the frequencies of each rotating component of the winch gear with respect to the shaft rotational frequency. The sign (-) means that the component turns in an opposite direction of the motor shaft.

Location	Components: frequency	Orders
First stage	Sun gear frequency 'fp1'	1x
	Planet Carrier frequency : 'fps1'	0.113 x
	Planet pass frequency : 'fs1'	-0.343 x
	Ring frequency : 'fc1'	-0.028 x
	Meshing frequency : 'Feng1'	10.64 x
Second stage	Sun gear frequency : 'fp2'	0.113 x
	Planet Carrier frequency : 'fps2'	0 x
	Planet pass frequency : 'fs2'	-0.079 x
	Ring frequency : 'fc2'	-0.028 x
	Meshing frequency : 'Feng2'	2.04 x

Table 1: Characteristic frequencies of the gear winch's components

4 Experimental Results

In this section we will apply the new method to real signals acquired from the winch benchmark.

4.1 Comparison results

In order to have a global outline of the effectiveness of the current analysis to detect gearbox wear, two spectra are compared. The first signal spectrum is referred as a reference acquired at the beginning of the ALT and the second signal is acquired at the end of the test. At this point, inspection and oil analysis have confirmed the gear degradation. Figure 7 presents a comparison of the two simple current spectra. It is noticeable that power in some frequency bands around the supply frequency has increased at the end of the ALT. This phenomenon is typically an amplitude modulation of the current supply frequency. The second stage in applying the new method is amplitude demodulation of the raw supply current. This will lead to extract the amplitude modulation function (AMF). Figure 8 presents the spectrum of the demodulated signal around the first supply frequency. Here also it is noticeable that some amplitude component has increased which can be used as an overall fault signature. Note that components that appear in the raw signal spectrum or the spectrum of the AMF cannot be well attributed and correlated to mechanical sources (see Table I) due to smearing caused by the winch velocity fluctuations.

By resampling the AMF using the instantaneous speed profile, an order spectrum is computed. Figure 9 presents this order spectrum computed around the fundamental supply frequency. We notice that the harmonic amplitudes of the first planet carrier frequency increases, which is also the frequency of the second stage sun gear frequency. This is a clear sign of the presence of abnormalities involving the degradation of

the gear. Figure 10 presents the order spectrums of the current AMF calculated by angular resampling of the demodulated current signal around the second supply frequency 'H2'. The comparison between the order spectrums at the beginning and the end of the ALT reveals that harmonic components related to the second stage sun gear frequency have increased considerably. Figure 11 presents a comparison of the order spectrum of the re-sampled FMA signal computed around the third harmonic of the supply frequency. Here also we can see that the presence of several harmonics of the sun gear frequency of the second stage confirms the presence of a mechanical fault concerning the input axis of the second stage or the planet carrier of the first stage since they are coupled.

4.2 Features extraction

The comparison results have shown an increase in amplitude of several harmonic of the first planet carrier frequencies of the gear components. Thus it is very important to quantify the increase of these amplitudes normalized with respect to the amplitude of the main carrier frequency (H1, H2 or H3 of the supply frequency). In fact the amplitude of the carrier frequency can be easily calculated as the dc component of the relative demodulated signal (Amplitude of the zero order components).

We can define a global modulation index as the ratio of the sum of amplitudes of the first 12 harmonics of the planet carrier frequency over the amplitude of the dc component, see equation (6).

$$GMI_x = \frac{\sum_{i=1}^{12} AHps\ 1_i}{H_0}, \quad x = 1,2,3 \tag{7}$$

With $AHps\ 1_i$ is the amplitude of i_{th} harmonic of the planet carrier frequency. x can take the values 1, 2 and 3, which designates respectively that the demodulation is done around the first, second and the third harmonic of the supply frequency.

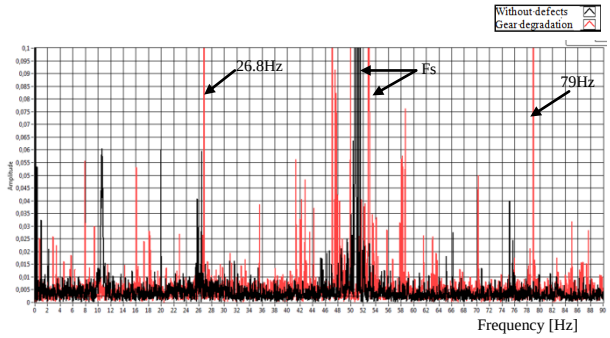

Figure 7: Frequency spectrum of the simple current in the band [0, 90] Hz.

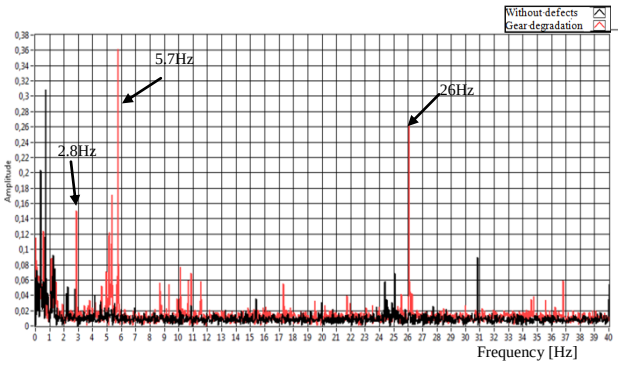

Figure 8: Frequency spectrum of the current AMF signal around the fundamental supply frequency [10,90] Hz.

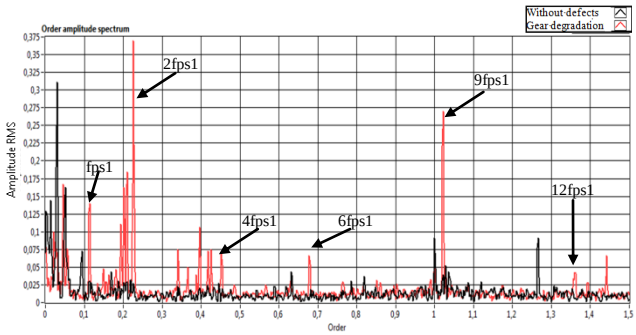

Figure 9: Order spectrum of the even angular spaced signal of the demodulated current around the fundamental supply frequency [10,90] Hz.

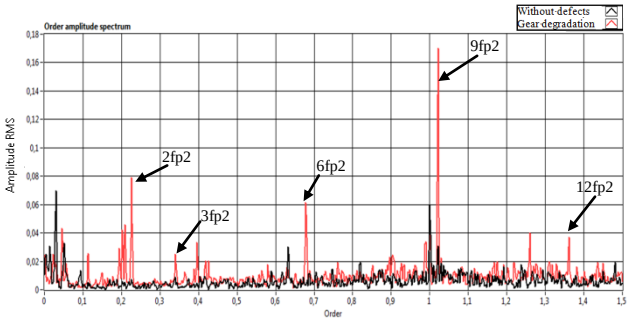

Figure 10: Order spectrum of the even angular spaced signal of the demodulated current around H2 of the supply frequency [60,140] Hz.

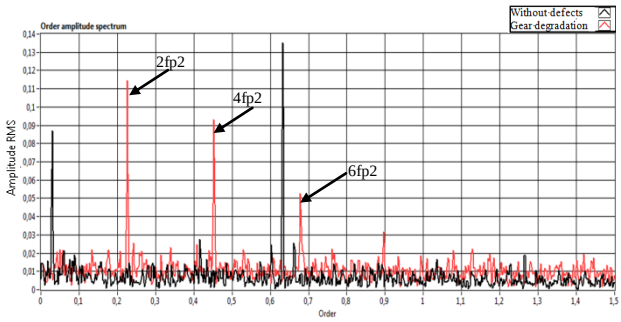

Figure 11: Order spectrum of the even angular spaced signal of the demodulated current around H3 of the supply frequency [110,190] Hz.

4.3 Features evolution over the ALT

In this section we present the evolution of some indicators extracted from the order spectrums of the current AMF during the ALT.

Figure 12 shows the evolution, over the whole duration of the ALT, of the global modulation index GMI1 calculated from the demodulated current signal around the first harmonic of the supply frequency. We can notice that this condition monitoring parameter increases linearly with respect to time and therefore with respect to the severity of the fault.

Figure 13 and Figure 14 show respectively the trend of the global modulation index GMI2 and GMI3. The GMI2 is calculated from the demodulated current signal around the second harmonic of the supply frequency while the GMI3 is calculated from the demodulated current signal around the third one. The trend of the GMI2 reveals that this condition monitoring parameter increases linearly with respect to the severity of the fault. The increase of this parameter is about 4% between the beginning and the end of the ALT. The trend of the GMI3 reveals that this indicator does not increase linearly as the two last GMI thus it can be simply used as a pertinent parameter.

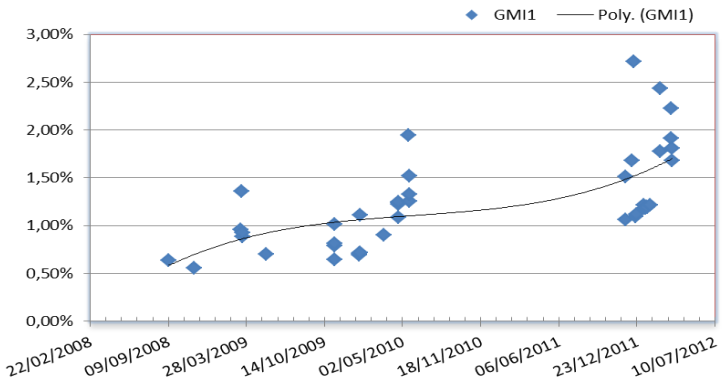

Figure 12: Evolution of the Global Modulation Index GMI1 over the ALT.

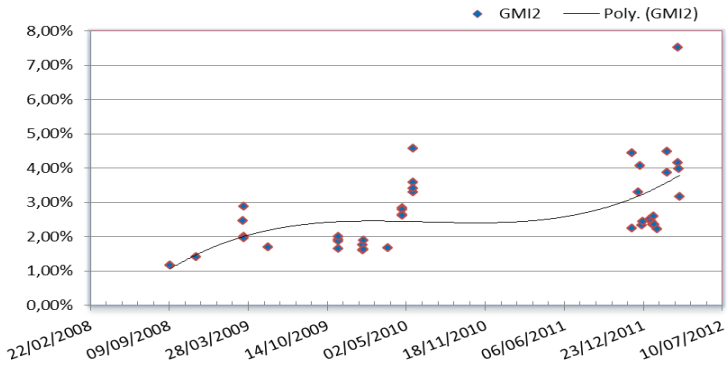

Figure 13: Evolution of the Global Modulation Index GMI2 over the ALT.

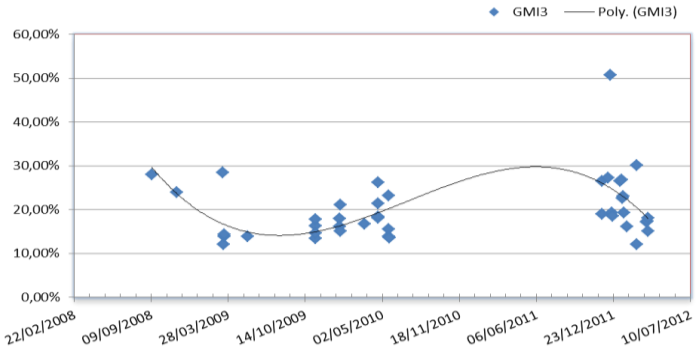

Figure 14: Evolution of the Global Modulation Index GMI3 over the ALT.

5 Conclusion

This paper shows the principal of a new diagnostic method based on current signal analysis by associating a demodulation technique with an angular resampling technique generally used for vibration signals. The performance of the new method is illustrated through experimental data coming from an accelerated life time test of a lifting crane. The lifetime test began on September 2008 and on February 2012 gear degradation has been clearly revealed by an oil analysis and inspection. Afterwards, condition monitoring indicators are defined. The results have shown that the first two indicators increase linearly with respect to time which proves the effectiveness of the new method to detect gear degradation.

Acknowledgments

The authors wish to thank the CETIM and specially the MLS committee for its technical and financial support.

References

[1] J.R. Cameron, W.T. Thomson, A.B. Dow, "Vibration and current monitoring for detecting airgap eccentricity in large induction motors," IEEE Proceedings, Vols. %1 sur %2133, Pt. B, No. 3,, pp. 155-163, 1986.

[2] R.R. Schoen ,T.G. Habetler, "Effects of Time-Varying Loads On Rotor Fault Detection In Induction machines," Industry Applications Society Annual Meeting, Conference Record of the 1993 IEEE, vol. 3, pp. 324-330, 1993.

[3] D.G. Dorrell, W.T. Thomson, Steven Roach, "Analysis of Airgap Flux Current And Vibration Signals as a Function of the Combination of Static and Dynamic Airgap Eccentricity in 3-Phase Induction Motors," IEEE Transactions on Industry Applications,, vol. 33, n° %11, pp. 24-34, Jan/Feb 1997.

[4] S. Nandi, H. Toliyat, "Condition monitoring and faults diagnosis of eletrical machines- A review," IEEE, pp. 197-204, 1999.

[5] M.E.H. Benbouzid, "A Review of Induction Motors Signature Analysis as a Medium for Faults Detection," IEEE TRANSACTIONS ON INDUSTRIAL ELECTRONICS, vol. 47, n° %15, pp. 984-993, 2000.

[6] M. Blodt, P. Granjon,B. Raison, G. Rostaing, "Models for Bearing Damage Detection in Induction MotorsUsing Stator Current Monitoring," IEEE International Symposium on Industrial Electronics, n° %1Ajaccio: France, 2004.

[7] M. Blodt, J. Faucher, B. Daques, M. Charbet, "Mechanical load fault detection in induction motors by stator current time-frequency analysis," IEEE International Conference on Electric Machines and Drives, pp. 1881-1888, 2005.

[8] A.R. Mohanty, C. Kar, «Fault Detection in a Multistage Gearbox by Demodulation of Motor Current Waveform,» IEEE TRANSACTIONS ON INDUSTRIAL ELECTRONICS, vol. 53, n° %14, pp. 1285-1297, 2006.

[9] M.Eltabach, J. Antoni, M. Najjar, "Quantitative analysis of noninvasive diagnostic procedures for induction motor drives," Mechanical Systems and Signal Processing 21, pp. 2838-2856, 2007.

[10] A. Ibrahim, M. El Badaoui, F. Guillet, F. Bonnardot, "A New Bearing Fault Detection Method in Induction Machines Based on Instantaneous Power Factor," IEEE Transactions on Industrial Electronics, vol. 55 No.12, pp. 4252-4259, Decembre 2008.

[11] J.Treetrong, «The use of higher-order spectrum for fault quantification of industrial electric motors,» Intelligent Control and Computer Engineering, vol. 70, p. 59-68, 2011.

[12] G.P. Arturo, R.-T. Rene de Jesus, «The application of high-resolution spectral analysis for identifying multiple combined faults in induction motors,» IEEE Transactions on Industrial Electronics, vol. 58, p. 2002-2010, 2011.

[13] N. Feki G. Clerc, Ph Velex, «An integrated electro-mechanical model of motor-gear units—Applications to tooth fault detection by electric measurements,» Mechanical System and Signal Processing, vol. 29, pp. 377-390, 2012.